Synthesis and Characterization of Novel Core-Shell Magnetic Nanogels Based on 2-Acrylamido-2-Methylpropane Sulfonic Acid in Aqueous Media

Ayman M. Atta

Petroleum Application Department, Egyptian Petroleum Research Institute, Nasr City 11727, Cairo, Egypt

Received 24 November 2010; accepted 20 June 2011
DOI 10.1002/app.35135
Published online 21 November 2011 in Wiley Online Library (wileyonlinelibrary.com).

ABSTRACT: Ultrafine well-dispersed Fe_3O_4 magnetic nanoparticles were directly prepared in aqueous solution using controlled coprecipitation method. The synthesis of Fe_3O_4/poly (2-acrylamido-2-methylpropane sulfonic acid) (PAMPS), Fe_3O_4/poly (acrylamide-*co*-2-acrylamido-2-methylpropane sulfonic acid) poly(AM-*co*-AMPS) and Fe_3O_4/poly (acrylic acid-*co*-2-acrylamido-2-methylpropane sulfonic acid) poly(AA-*co*-AMPS) -core/shell nanogels are reported. The nanogels were prepared via crosslinking copolymerization of 2-acrylamido-2-methylpropane sulfonic acid, acrylamide and acrylic acid monomers in the presence of Fe_3O_4 nanoparticles, *N,N′*-methylenebisacrylamide (MBA) as a crosslinker, *N,N,N′,N′*-tetramethylethylenediamine (TEMED) and potassium peroxydisulfate (KPS) as redox initiator system. The results of FTIR and ^{1}H-NMR spectra indicated that the compositions of the prepared nanogels are consistent with the designed structure. X-ray powder diffraction (XRD) and transmission electron microscope (TEM) measurements were used to determine the size of both magnetite and stabilized polymer coated magnetite nanoparticles. The data showed that the mean particle size of synthesized magnetite (Fe_3O_4) nanoparticles was about 10 nm. The diameter of the stabilized polymer coated Fe_3O_4 nanogels ranged from 50 to 250 nm based on polymer type. TEM micrographs proved that nanogels possess the spherical morphology before and after swelling. These nanogels exhibited pH-induced phase transition due to protonation of AMPS copolymer chains.
 J Appl Polym Sci 124: 3276–3285, 2012

Key words: core-shell magnetic nanogels; 2-acrylamido-2-methylpropane sulfonic acid; acrylamide copolymers; polymerization; aqueous solution

INTRODUCTION

Magnetite Fe_3O_4 powders, which are nontoxic at certain concentrations and could be easily synthesized, have been intensively investigated. Magnetic nanoparticles possess some extraordinary physical and chemical properties and find applications in many industrial and biological fields.[1–4] Magnetic nanoparticles also find applications in making membranes, generating electricity, and fabricating memorizer for electronic and quantum computers.[1] The preparation methods of magnetite powders mainly include coprecipitation,[1,2] microwave thermal-hydrolysis,[3] oxidation of $Fe(OH)_2$ by H_2O_2,[4] ultrasonic irradiation,[5] micron-scale capsule,[6] and thermal decomposition of $Fe(CO)_5$.[7] Because of the high ratio of surface to volume and magnetization, Fe_3O_4 nanoparticles are prone to aggregate. To enhance the compatibility between the magnetic Fe_3O_4 nanoparticles and water, and to control and/or tailor of the surface properties of the nanoparticles, the surface modification for magnetic Fe_3O_4 nanoparticles is a necessity. However, it is reported that the saturation magnetization of nanoparticles was much lower than that of correspondent bulk sample and decreased along with the reduction of the particle size.[8]

The superparamagnetic Fe3O4 nanoparticles coated with polymers are usually composed of the magnetic cores to ensure a strong magnetic response and a polymeric shell to provide favorable functional groups and features.[9] Polymeric coating materials can be classified into synthetic and natural. Polymers based on poly(ethylene-*co*-vinyl acetate), poly(vinylpyrrolidone) (PVP), poly(lactic-*co*-glycolic acid) (PLGA), poly(ethylene glycol) (PEG), poly (vinyl alcohol) (PVA), etc. are typical examples of synthetic polymeric systems.[10] Natural polymer systems include use of gelatin, dextran, chitosan, pullulan, etc.[11] The natural polymers modification offers significant advantages in biomedicine application due to their good biocompatibility and degradability.[10] Several methods have been developed to synthesize magnetic nanoparticles, such as microemulsion polymerization,[12,13] reverse microemulsion,[14] *in situ* polymerization[15] and suspension crosslinking method,[16] etc. However, these processes were

Correspondence to: A. M. Atta (khaled_00atta@yahoo.com).

conducted in a water/oil system, and usually involved surfactants and emulsifying agents, which made the magnetic nanoparticles difficult to solubilize or stabilize in aqueous system, and then posed limitations to practical biomedical applications, particularly for *in vivo* applications In this article, we propose an alternative approach to synthesize polyacrylamide (PAM) superparamagnetic nanogels based on 2-acrylamido-2-methylpropane sulfonic acid (AMPS), acrylic acid (AA) and acrylamide (AM) via solution polymerization at room temperatures in an initiator free aqueous system. Also the pH-sensitivity of the hybrid nanogels was investigated.

EXPERIMENTAL

Materials

All chemicals were of analytical grade, commercially available and used without further treatments, except that 2-acrylamido-2-methylpropane sulfonic acid (AMPS), acrylic acid (AA) and acrylamide (AM), from Aldrich chemicals, have been purified or recrystallized prior to use. *N,N*$^{-}$-methylene-bis(acrylamide), which served as crosslinker, was supplied by Aldrich chemicals *N,N,N′,N′*-tetramethylethylenediamine (TEMED) were all purchased from Aldrich Chemical; potassium peroxydisulfate (KPS) was used without further purification. N_2 (99.99%) was used as protective gas. Deionized water was used in the experiment.

2-acrylamido-2-methylpropane sulfonic acid sodium salt (AMPS-Na) stock solution was prepared by dissolving 20 g of AMPS in about 40 mL of deionized water and adding to this solution 10 mL of a 30% NaOH solution under cooling. Then, the solution was titrated with 1*M* NaOH to pH. 7 : 00 and finally, the volume of the solution was completed to 100 mL with deionized water. AMPS-Na stock solution (1 mL) of thus prepared contained 0.966 mmol AMPS-Na.

Preparation of Fe_3O_4 nanoparticles

Fe_3O_4 nanoparticles were prepared by the partial reduction method according to Ref. 17, as shown in eq. (1):

$$6Fe^{3+} + SO_3^{2-} + 18NHO_4OH \rightarrow 2Fe_3O_4 + SO_4^{2-} + 18NH_4^{+} + 9H_2O \quad (1)$$

Fe_3O_4 nanoparticles are prepared as follows: 6 mL of 1 moldm^{-3} ferrous chloride solution was diluted with 50 mL of deionized water under N_2 to keep oxygen free throughout the preparation procedure. The solution was mixed dropwise with 3 mL of 0.1 mold m^{-3} sodium sulfite solution into reaction flask. Ammonia solution, 4 mL of 28% diluted 20 mL water, was added quickly into the prepared ferrous solution under mechanical stirring. The flask was kept at 180°C for 6 h, and allowed to cool to room temperature. The black magnetic precipitates were recovered in an external magnetic field and washed several times with distilled water, and washed again with (2 : 1) water-ethanol solution. The resulted Fe_3O_4 nanoparticles were pulverized together with alcohol.

Preparation of polymeric-coated magnetic nanogels

The polymeric-coated magnetic nanogels were obtained by solution polymerization technique. The Fe_3O_4 nanoparticles were at last redispersed in deionized water, and adjusted (pH = 2) with 2 mol/L HCl. The concentration of the Fe_3O_4 nanoparticles was adjusted to 10 mg/mL. Fe_3O_4 nanoparticles were dissolved 85 mL deionized water and dispersed using ultrasonic for 3 min and heated at 45°C. Then different amount of AMPS, AMPS-Na, AA/AMPS, or AM/AMPS (1–3 wt %) was added to the solution. The molar ratio between AMPS:AA or AMPS: AM was 96 : 4 mol %. The solution was purged with N_2 for 30 min, then 4.0 mmol MBA, 0.4 mmol KPS, and 0.67 mmol TEMED were added into the solution to carry out polymerization for 15 h at 45°C. The polymer-modified Fe_3O_4 particles were collected in an external magnetic field. They were washed with distilled water three times and dispersed in deionized water in an ultrasonic device.

The prepared PAMPS and PAMPS-Na polymers were designated as PAMPS-1, PAMPS-2, and PAMPS-3 at monomer concentrations 1, 2, and 3 wt %, respectively. The same numbers were used to designate AA/AMPS and AM/AMPS crosslinked copolymers.

Characterization

Structures of the magnetic nanogels were analyzed with a Nicolet FTIR spectrophotometer in a wave number range of 4000–500 cm^{-1} with a resolution accuracy of 4 cm^{-1}.

Chemical structures of these nanogels are measured by ^{1}H-NMR techniques. Samples for ^{1}H-NMR are prepared as follows: the nanogels particles were and redispersed in D_2O solvent. Their spectra are recorded on a Bruker NMRSpectrometers: avance DmX-500 at 25°C.

Micrographs of the colloidal nanogel particles were taken using a H-800 transmission electron microscope (TEM). The sample was prepared by

adding acetone to the aqueous solution of nanogels till the solution became slightly turbid.

Transparency measurements were performed using a Unicam SP 1800 ultraviolet spectrophotometer at an operating wavelength λ_{max} (ε) = 500 nm in optically homogeneous quartz cuvettes. The concentration of the solutions was 0.70 mg/mL.

The pH of solutions was adjusted with very small amounts of 0.1*M* hydrochloric acid and sodium hydroxide using a digital pH meter (pHS-4CT, Shanghai Dazhong Analytical Instrument). The ionic strength of solutions was adjusted to be 0.1*M*.

RESULTS AND DISCUSSION

Several types of iron oxides exist in nature and can be prepared in the laboratory, but nowadays only maghemite (-Fe_2O_3) and magnetite (Fe_3O_4) are able to fulfill the necessary requirements for different applications. These requirements include sufficiently high magnetic moments, chemical stability in physiological conditions and low toxicity, not to mention the easy and economical synthetic procedures available for the preparation of these materials. The degree of atomic order in the iron oxide lattice, or in other words its degree of crystallinity, as well as the dispersity in terms of size and shape of the nanoparticles are critical parameters that affect their performance in medical application. These parameters are strongly correlated to the approach followed for their preparation. Several synthetic procedures have been developed to synthesize iron oxide nanoparticles.[18] The simplest, cheapest and most environmentally friendly procedure is based on the coprecipitation method, which involves the simultaneous precipitation of Fe^{2+} and Fe^{3+} ions in basic aqueous media [19–21].

In the coprecipitation method the reaction temperature is limited by the boiling point of water, and iron oxide nanoparticles synthesized under these conditions exhibit usually a low degree of crystallinity and large polydispersity. An improvement in this direction was represented by the synthesis routes employing water-in-oil microemulsions.[22] In these approaches, a certain amount of water is added to a large amount of nonpolar solvent (oil) and, in the presence of appropriate amphiphilic surfactant molecules, homogeneously distributed droplets of water stabilized by the surfactant molecules act as micro or nano-reactors for the nucleation and controlled growth of iron oxide nanoparticles. In these syntheses an improvement in the dispersity of the particles was reported, due to the size confinement offered by the water pool inside each micelle. Even in these cases however the limited reaction temperature achievable leads to a low crystallinity of the material and additionally the products are obtained in low yields. In this respect, the present articles discussed the formation of crosslinked magnetic Fe_3O_4 core AMPS, AM/AMPS, and AA/AMPS shells. Fe_3O_4 nanoparticles were prepared by partial reduction of ferric ion by using sodium sulfite as a moderate reducing agent and succeeding coprecipitation by diluted ammonium hydroxide. It was proposed that AMPS, AMPS-Na, AM, and AA monomers and MBA crosslinker were adsorbed on the modified Fe_3O_4 particle through chelation between Fe_3O_4 and the sulfur, oxygen and nitrogen atoms of monomers. The proposed preparation scheme of crosslinking polymerization of AMPS, AMPS/AA, and AMPS/AM was shown in Scheme 1. The high specific surface areas of Fe_3O_4 nanoparticles resulted in their strong adsorption ability,[23] so the crosslinked polymers were polymerized onto the surface of the magnetic nanoparticles by a free-radical polymerization in the presence of MBA crosslinker. The monomers and crosslinker were prone to be adsorbed on Fe_3O_4 surface primarily. Additionally, the molar extinction coefficient of nano-sized Fe_3O_4 at 45°C was much larger than that of AMPS, AM, and AA or MBA molecules in solution, so when the system was thermally heated at 45°C, Fe_3O_4 nanoparticles were thought to absorb the vinyl monomers and MBA molecules on the surface of Fe_3O_4 nanoparticles which were activated and polymerized. It was expected that AM, AA, and AMPS functionalized magnetic nanogels synthesized via thermal polymerization would be a core-shell structure, where nanosized Fe_3O_4 was the core and PAMPS, PAMPS-NA, AMPS/AA, and AMPS/AM formed the amino-functionalized hydrophilic gel shell. The adsorption of AMPS, MBA, AM, and AA as ligand onto Fe_3O_4 colloidal nanoparticles clusters has been studied by means of FTIR, H-NMR, TEM, and XRD analyses.

Characterization of the crosslinked nanogels

To understand binding and crosslinking of Fe_3O_4-PAMPS, PAMPS-Na, AM/AMPS, and AA/AMPS nanogels s during polymerization, FT-IR spectra of the hydrogels were evaluated and are presented in Figure 1. The chemical structure of Fe_3O_4 modified nanoparticles was proved using FTIR analysis. In this respect, the FTIR spectrum of Fe_3O_4 was represented in Figure (1a). The bands between 2800 cm^{-1} and 3000 cm^{-1} shown in Figure 1(a) could be attributed to the flex vibrations of -CH_2, indicating that surface modification of Fe_3O_4 nanoparticles was successful. The experimental results indicated that the improved method proposed to prepare Fe_3O_4 nanoparticles was reasonable. The bands at 576 and 470 cm^{-1} related to Fe-O group indicated the formation of Fe_3O_4. The chemical structures of coated Fe_3O_4 nanoparticles with AMPS -Na, AMPS, AA/

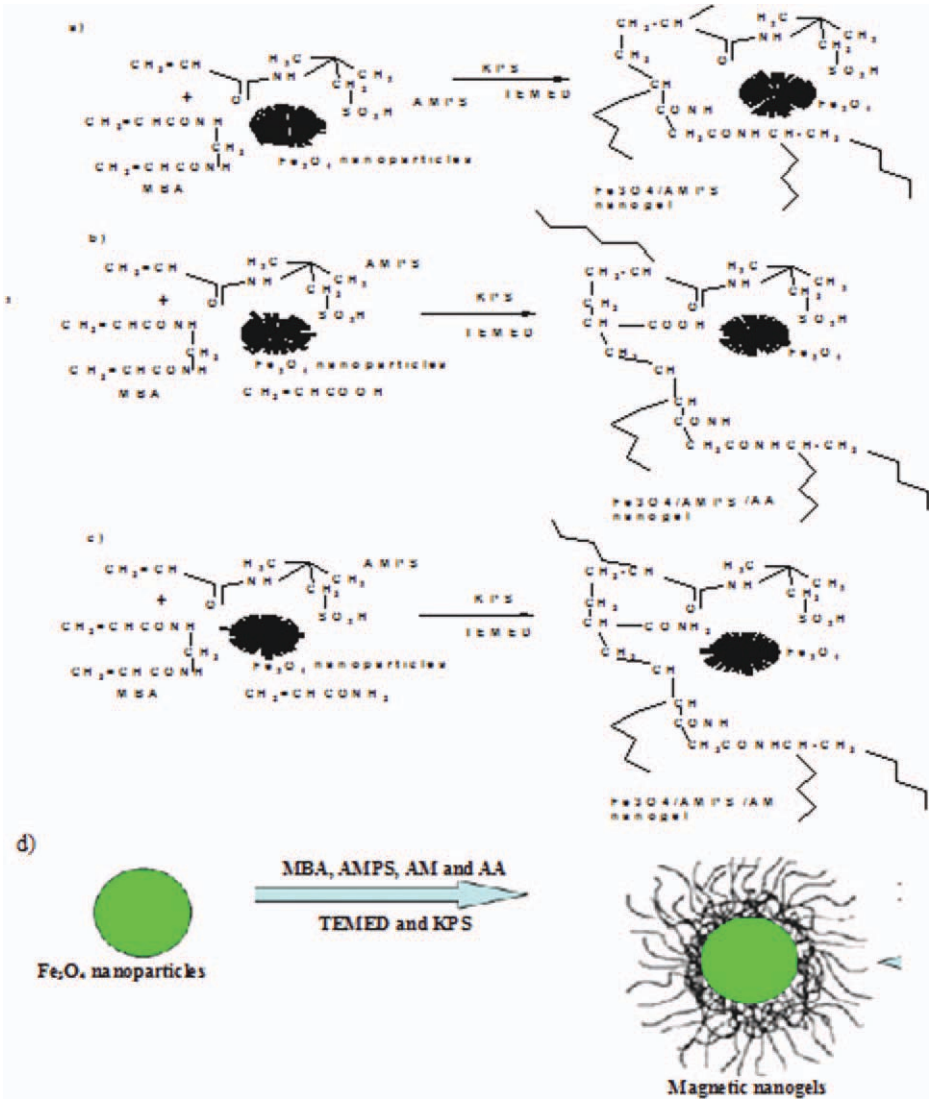

Scheme 1 Crosslinking polymerization of (a) Fe_3O_4/AMPS, (b) Fe_3O_4/AMPS/AA, (c) Fe_3O_4/AMPS/AM, and (d) Fe_3O_4 core/shell nanogels. [Color figure can be viewed in the online issue, which is available at wileyonlinelibrary.com.]

AMPS, and AM/AMPS polymers were illustrated by FTIR. The FTIR spectra of PAMPS and Fe_3O_4-PAMPS and Fe_3O_4-AA/AMPS nanogels were selected and represented in Figure 1(b–d), respectively. In the FT-IR spectra of the hydrogels, the bands at about 1700 and 3100–3500 cm^{-1} are important. The bands at about 1600–1700 cm^{-1} could be attributed to a shift in stretching vibration associated with hydrogen that is bonded directly to an overtone of the strong carbonyl absorption. The peak at 1650–1660 cm^{-1} is the carbonyl group and related to amide groups and at 1500–1600 cm^{-1} is the *N*—H bonding vibration. The much broader absorption peaks in the regions of 3100 cm^{-1} and 3500 cm^{-1} are *N*—H bands and related to "polymeric" bands. The broad peak 3500 is characteristic peak of primary amine. On the other hand, it is thought that the peaks at 1200 cm^{-1} are C—N bands, and the peaks at 2850 cm^{-1} and 1400 cm^{-1} show —CH_2— groups on the polymeric chain. Two typical peaks of C—H vibrations of —$CH(CH_3)_2$ can be at 1380–1385 cm^{-1}. The characteristic absorption peak of AMPS units is shown at 1040 cm^{-1} due to SO group.[24] The peaks observed in the FT-IR spectra confirm the presence of AM and AMPS. Careful inspection of FTIR spectra indicates that the disappearance of bands at 3050, 1600, and 950 cm^{-1} which attributed to =CH stretching, C=C stretching, and =CH (out of-plan-bending), respectively; refers to the complete polymerization of monomers and MBA crosslinker. The absorption bands at 1457 cm^{-1} and 2925 cm^{-1} are observed in all spectra which attributed to CH_2 asymmetric bending and asymmetric stretching respectively. On the other hand, the absorption bands at 1394 cm^{-1} and 2855 cm^{-1} can be referred to CH_3 symmetric bending and symmetric stretching

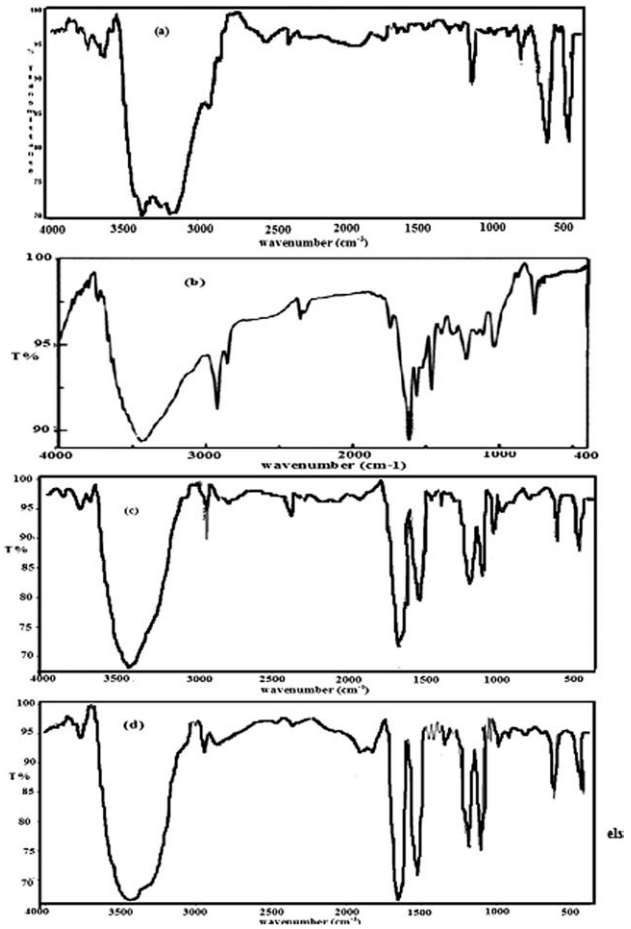

Figure 1 FTIR spectra of (a) Fe_3O_4, (b) PAMPS, (c) Fe_3O_4-PAMPS1, and (d) Fe_3O_4-AA/AMPS1 crosslinked with MBA.

of AMPS monomer. The absorption bands at 618, 1034, and 1223 cm^{-1} appeared in the spectrum are assigned to the S—O stretch, S=O asymmetric stretch, and symmetric stretch of sulfonic acid groups respectively. In the FTIR spectra of magnetic Fe_3O_4-PAMPS, PAMPS-Na, AA/AMPS, and AM/AMPS magnetic nanogels, the bands of Fe_3O_4 between 540 and 650 cm^{-1} demonstrate the existence of Fe_3O_4 in the magnetic nanoparticles. The absorption band of 1650 cm^{-1} was attributed to the C=O stretching vibrations of carbonyl group of MBA, which served as a crosslinker in the crosslinking polymerization. Careful inspection of FTIR spectra indicates that the disappearance of bands at 3050, 1600, and 950 cm^{-1} which attributed to =CH stretching, C=C stretching, and =CH (out of-plan-bending), respectively; refers to the complete polymerization of monomers and MBA crosslinker. The bands of 1680, 1590, and 1384 cm^{-1} were assigned to CONH stretching, NH bending, and C—N stretching vibration, respectively, indicated the formation of crosslinked PAMPS [Fig. 1(b)]. In the spectrum of PAMPS nanogels [Fig. 1(c)], compared with the spectrum of PAMPS, the 1680 cm^{-1} peak of CONH shifted to 1700 cm^{-1}, 1596 cm^{-1} band of *N*—H bending vibration shifted to 1613 cm^{-1}, the 1384 cm^{-1} peak of —C—N bending vibration shifted to 1392 cm^{-1}, and a new sharp band 584 cm^{-1} appeared, and could be seen from Figure 1 that all characteristic peaks of PAMPS were also present in the spectrum of Fe_3O_4-PAMPS nanogels. The results indicated that PAMPS, PAMPS-Na, AMPS/AA, and AMPS/AM were coated on Fe_3O_4 nanoparticles successfully.

Similar conclusions can be made from the ^{1}H-NMR spectra. The spectra of Fe_3O_4/PAMPS-Na1, Fe_3O_4/AM/AMPS1, and Fe_3O_4-AA/AMPS1 nanogels were selected and represented in Figure 2. The disappearance of peaks at 5.8–6.3 ppm which attributed to CH_2=CHCO of monomers and appearance of new peaks at 0.8–1.2 ppm indicated the complete crosslinking polymerization of monomers and crosslinker. The peaks between 0.8 and 1.2 ppm are assigned to the methyl and methylene polymerization hydrogens in the molecular formula in Scheme 1. The peaks at 3.62 and 2.28 ppm (Fig. 2) are attributed respectively, to the protons of methylene group and methyl group of -$C(CH_3)_2CH_2SO_3^-$ in the AMPS molecule. On the other hand the peak at 5.5 ppm

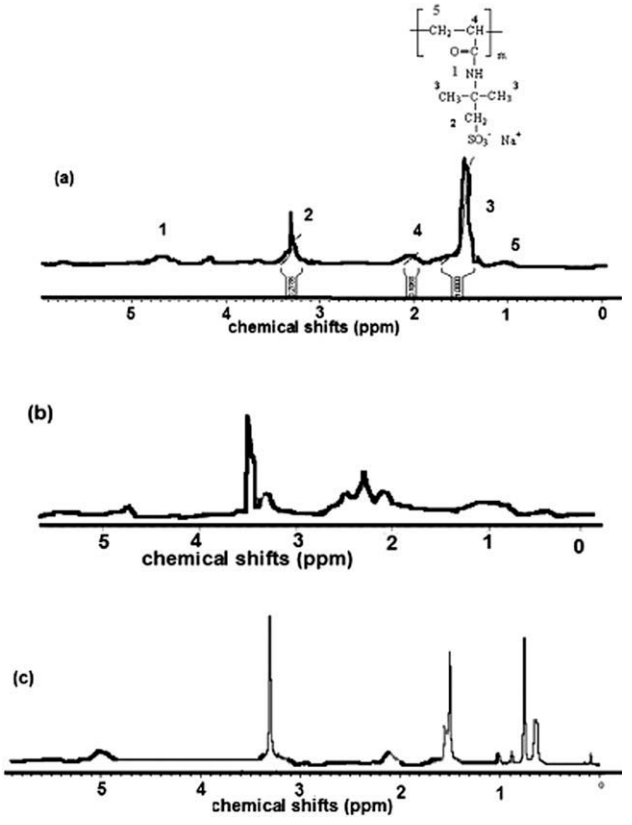

Figure 2 ^{1}H-NMR spectra of (a) Fe_3O_4-PAMPS-Na1, (b) Fe_3O_4-AM/AMPS1, and (c) Fe_3O_4-AA/AMPS nanogels in D_2O at 25°C.

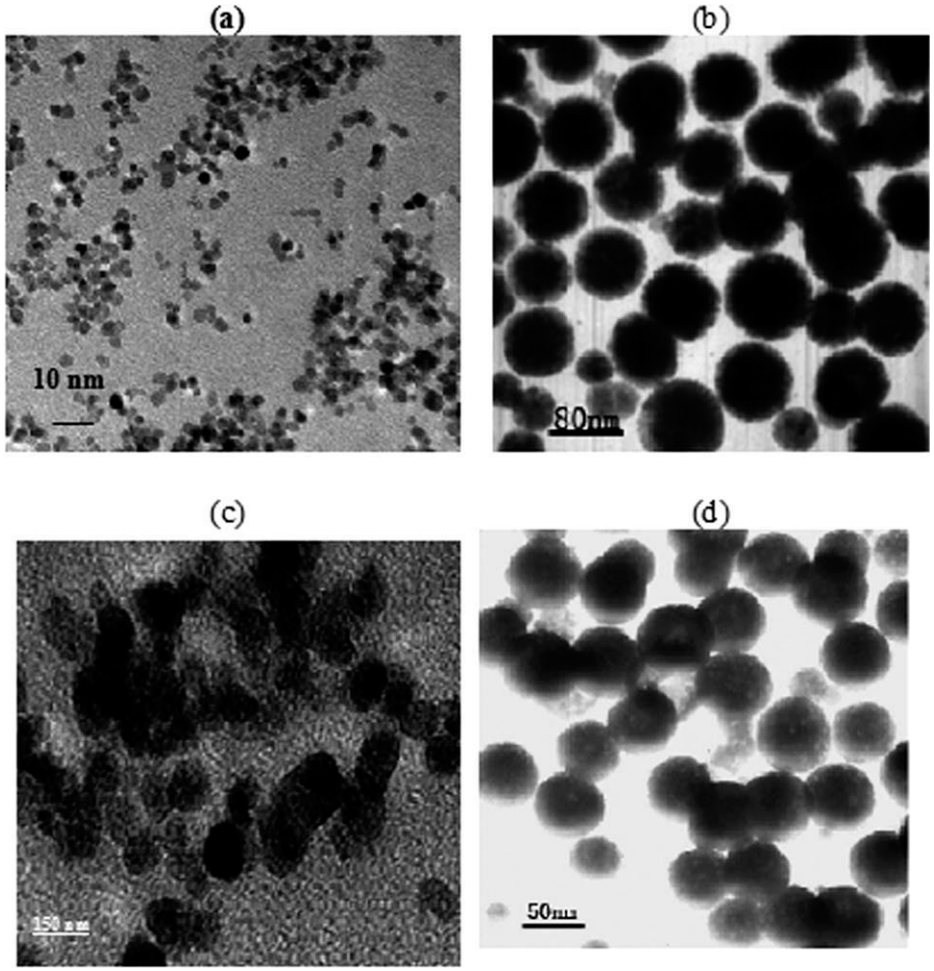

Figure 3 TEM photos of (a) Fe_3O_4, (b) Fe_3O_4-PAMPS-Na, (c) Fe_3O_4-AM/AMPS1, (d) Fe_3O_4-AA/AMPS1.

can be attributed to -CONH- of AMPS. The results prove that AMPS is found in the prepared polymers.

Morphologies of AMPS polymer magnetic nanogels

To know better the structure of magnetic nanogels, their morphologies were observed by TEM images. The TEM images of Fe_3O_4, Fe_3O_4-PAMPS-Na, Fe_3O_4-AM/AMPS, and Fe_3O_4- AA/AMPS nanogels were represented in Figure 3(a–d), respectively. As shown in Figure 3(a), monodispersed magnetic nanogels and Fe_3O_4 nanoparticles exhibited uniform spherical shape, and narrow particle-size distributions. The mean particle size of naked Fe_3O_4 nanoparticles was about 10 nm as calculated from Figure 3(b).

The diameter of the Fe_3O_4/PAMPS-Na1 and Fe_3O_4-AA/AMPS1 nanogels is about 50 and 80 nm, respectively. The nanoparticles are rough and the brim is transparent. The diameters of Fe_3O_4/AMPS/AM1 nanogels were in the range of 150–200 nm. Comparing the TEM images of Fe_3O_4-PAMPS-Na and Fe_3O_4-AA/AMPS nanogels, Figure 2(b,d), with image of Fe_3O_4-AM/AMPS nanogels shows that microspheres of Fe_3O_4- PAMPS-Na and Fe_3O_4-AA/AMPS were more monodisperse and much smaller than those for Fe_3O_4-AM/AMPS nanogels. It is well known that, to design complex and versatile nanogels, it is often desired that the particles have nanogel surface with multiple functional groups for covalent bonding attachment in the postpolymerization stage.[24,25] For example, the presence of carboxyl and amine groups on the same particle surface can limit the extensively used carbodiimide-based amides for chemoligation, as a result of cross-reaction of both functional groups.[26] Accordingly, the presence of both SO_3^{-2} and COO^- ionic groups in the structure of AMPS/AA nanogels increased their dispersion in the aqueous medium which increased the formation of monodispersed nanogels. In the case of acrylamide monomers (AMPSA and AM) capable of formation of stable hydrogen bonds, this suggests aggregation of the monomers. The aggleomeration of the prepared nanogels increased the diameter of AMPS/AM nanogels.[27]

TEM was carried out to study the variation of size, morphology, and core shell structure of the nanogels with variation of monomers content. In this

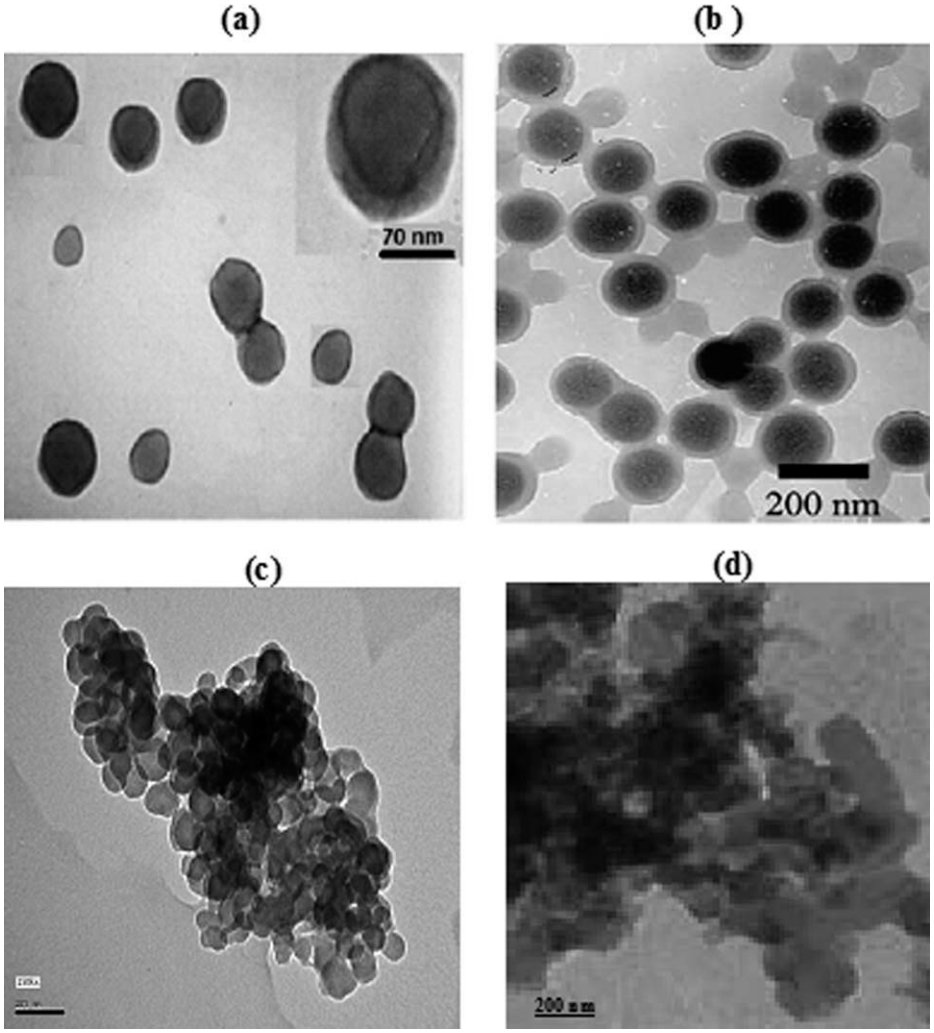

Figure 4 TEM photos of (a) Fe_3O_4-AA/AMPS3, (b) Fe_3O_4-AM/AMPS3, (c) Fe_3O_4-PAMPS1, and (d) Fe_3O_4-PAMPS3.

respect, TEM images of PAMPS, PAMPS-Na, AMPS/AA, and AMPS/AM having monomers content 3 wt % were represented in Figure 4. The average particle size diameters of the prepared nanogels were determined and listed in Table 1. In this respect, the particle diameters of Fe_3O_4- PAMPS1, PAMPS-Na1, AMPS/AA1, and AMPS/AM1 were 100, 50, 75, and 150 nm, respectively. The diameters of Fe_3O_4-PAMPS3, PAMPS-Na3, AMPS/AA3, and AMPS/AM3 were 200, 40, 80, and 250 nm, respectively. A close examination of the TEM image (inset in Figs. 3 and 4) reveals the presence of MNPs at the center with a PAMPS, PAMPS-Na, AMPS/AA, and AMPS/AM coating surrounding them. The size of the magnetic core was similar to earlier reported values of MNPs synthesized by similar methods.[28] The decrement of agglomeration and size of nanogels with decreasing monomer concentrations might be a result of the electrostatic charge repulsion from the amine group of AMPS which would further reduce the magnetic dipole interactions and promote stability.[28,29] On the other hand, increment of monomer concentrations decrease the probability to surround the Fe_3O_4 particles due to decreasing of both crosslinker and Fe_3O_4 concentrations which decrease the dispersability of MNPs and consequently increase the size of nanogelss. The enlarged inserted

TABLE I
Average Particle Size Diameters of the Prepared Nanogels

Polymer designation	Monomers content (wt %)	Average particle diameters (nm)
Fe_3O_4-PAMPS-Na	1	50
	2	40
	3	30
Fe_3O_4-PAMPS	1	100
	2	125
	3	200
Fe_3O_4-AMPS/AA	1	70
	2	75
	3	80
Fe_3O_4-AMPS/AM	1	150
	2	180
	3	250

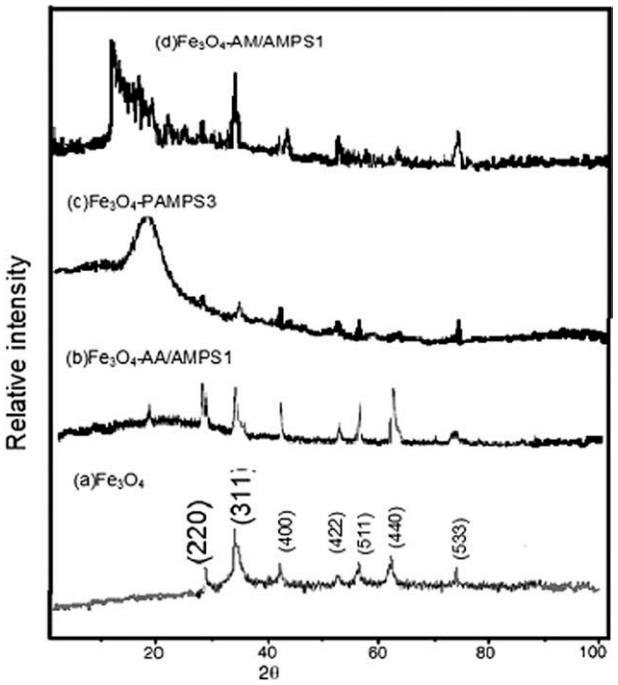

Figure 5 XRD of the prepared nanogels.

figures in Figures 3 and 4 showed that the dark region was wrapped by the white cloud, which confirmed the core-shell structure of the obtained magnetic nanogels.[30]

XRD analysis

X-ray powder diffraction was used to identify the as prepared nanogels, and the pattern is illustrated in Figure 5. The X-ray powder diffraction pattern shown in Figure 3 was measured at room temperature for all the samples. Figure 5(a) shows the XRD spectra of Fe_3O_4 nanoparticles prepared by the coprecipitation method. The figure shows only the characteristic peaks of Fe_3O_4 without interference from other phases of Fe*x*O*y*, to indicate the high purity of the Fe_3O_4 obtained. In addition, the peaks were widened, implying the small size of the particles. By comparing with XRD card 03-065-3107, it appears that antispinel Fe_3O_4 was synthesized. The XRD pattern of Fe_3O_4 particles shows main peaks at 2 of 30°, 35°, 42°, 54°, 57°, and 62.5°, corresponding to (220), (311), (400), (422), (511), and (440) Bragg reflection, respectively. There are a series of characteristic peaks: d = 2.964 (220), 2.525 (311), 2.092 (400), 1.717 (422), 1.612(511), 1.478 (440), and 1.276. (533) The d values calculated from the XRD pattern, according to the equation $d = \lambda/2$ sin, are well indexed to the inverse cubic spinel phase of Fe_3O_4. The average crystallite size D is calculated to be 15 nm, using the Debye-Sherrer formula $D = K\lambda/(\beta \cos)$, where K is the Sherrer constant (K = 0.89), λ the X-ray wavelength (λ = 1.5406A°), b the peak width of half maximum, and the Bragg diffraction angle.[31] The Debye-Scherrer calculations predict an average diameter of 15 nm for particles, which is smaller than the radius measured by TEM.

Figure 5(b) showed the XRD patterns for the naked and Fe_3O_4 nanoparticles coated with AA/AMPS1. Six characteristic peaks for Fe_3O_4 marked by their indices [(2 2 0), (3 1 1), (4 0 0), (4 2 2), (5 1 1), and (4 4 0)] were observed for both samples. It is also explained that the coating process did not result in the phase change of Fe_3O_4. The broad nature of the diffraction bands in the pattern below is an indication of small particle size, so the particle sizes can be quantitatively evaluated from the XRD data using the Debye-Scherrer equation. The Fe_3O_4 nanoparticles coated with AA/AMPS1 has average diameter of 35 nm. The XRD pattern of the magnetic Fe_3O_4-PAMPS3 was represented in Figure 5(c). The PAMPS nanogelss are consistent with the patterns of Fe_3O_4 particles, which indicate that a portion of the Fe_3O_4 particles diffused into the magnetic Fe_3O_4-PAMPS nanogels. The highest peak was attributed to PAMPS.

The XRD patterns of Fe-AM/AMPS3 was selected and represented in Figure 5(d). The fits to the X-ray patterns are composed of three phases as seen in Figure 5(d). The sharp component around 45.1 is attributed to the crystalline bcc a-Fe phase, the broad peak to an amorphous phase[32] and the shoulder around which is centered on 35.1 is due to an iron (Fe) oxide phase. The amorphous phase initially increases slightly and then decreases as the smaller particles oxidize more; finally, the oxide phase steadily increases as the surface oxidation increases with the increase in surface-to-volume ratio of particles. The presence of a broad peak in XRD measurement may be due to amorphous nature or the nano crystalline nature of the AM/AMPS sample.

Transmittance measurements

AMPS received attention in recent years due to its strongly ionizable sulfonate group. The synthesis of AMPS copolymers via radical chain polymerization is a well-established procedure. AMPS dissociate completely in the overall pH range, and therefore, the hydrogels derived from AMPS exhibit pH independent swelling behavior. Crosslinker molecules can be incorporated into chains simultaneously and form a permanent link between them. Polyelectrolyte hydrogels are based on charged networks that contain ionized groups. Negatively or positively charged hydrogels usually exhibit different degrees of equilibrium swelling at different pH values depending on the ionic composition of the polymers. Conventional pH-sensitive polymers are mostly

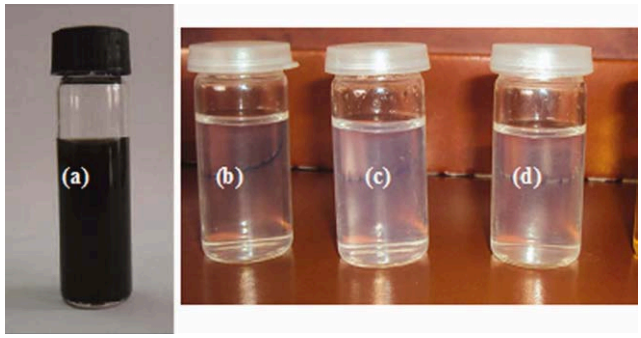

Figure 6 Photos of (a) Fe_3O_4, (b) Fe_3O_4-PAMPS-Na, (c) Fe_3O_4-AM/AMPS1, (d) Fe_3O_4-AM/AMPS3 solutions. [Color figure can be viewed in the online issue, which is available at wileyonlinelibrary.com.]

based on those containing ionizable groups of a base (amino group). Since PAMPS is a strong organic acid and is in the molecular state at pH < pKa = 3,[33,34] there is a strong hydrogen bonding between the SO_3H group of the PAMPS and -CONH group of the AM. Crosslinked PAMPS, P-AMPS-Na nanogels form colloid dispersions in neutral condition. These colloid dispersions are opalescent systems; the transmittance values vary between 45 and 95% at neutral pHs. The transmittance of aqueous colloid systems containing crosslinked PAMPS-Na, PAMPS, AA/AMPS and AM/AMPS nanogels was evaluated in deionized water at pH 6.5. Clear or opaque aqueous colloid systems were produced and were stable at room temperature for several days. In this respect photographs of the prepared nanogels were represented in Figure 6. It was observed that the transmittance of crosslinked particles increased by increasing the pH and decreasing the crosslinker contents (Wt%). Figure 8 summarizes the transmittance of the various nanogels composed of different weight percentages of AMPS, AA and AM crosslinked with MBA at different crosslinking ratios. This trend has been observed, caused by the different swellability of nanogels depending on the permeability of crosslinked particles by the solvent molecules and the different commensurability of the size of nanogels with the operating wavelength. It was also observed that, the transmittance increased for PAMPS-Na > AA/AMPS > PAMPS > AM/AMPS. This can be attributed to residual carboxyl groups of AA chains and sulfonate groups of AMPS deprotonate by increasing the pH; the particles become more compact; therefore, the ratio of particle size and the wavelength changes caused rising transmittance values. Figure 7 demonstrates that the transmittance of the nanogel dispersions increased with the increase of the pH value. It is found that the transmittance of PAMPS nanogels rises sharply at pH 4-4.5 for PAMPS-Na, 4.5-5 for AA/AMPS 6.5-7.0 for PAMPS, and pH 8.5-9 for AM/AMPS. At low pH, there is a very strong hydrogen bonding between the polymer chains of nanogels in aqueous solution thus leading to low transmittance. As pH increases, PAMPS becomes ionized, and the ionized PAMPS weakened the H-bonding between AMPS and AA or AM and strengthened the water-solubility of particles swell and the nanogels dispersion becomes transparent. At lower ratio of the crosslinker, the swellability of the colloid dispersion was greater, and the aqueous systems were clear, caused by the deprotonation of free carboxyl and sulfonate groups of the polymer chains. An increasing ratio of crosslinker corresponds to decreasing the amount of residual carboxyl and sulfonate groups of AA and AMPS; the particles became more compact; therefore, the opalescence of solutions increased.

CONCLUSIONS

The results indicated that PAMPS, PAMPS-Na, AMPS/AA, and AMPS/AM were coated on Fe_3O_4 nanoparticles successfully. TEM indicated that monodispersed magnetic nanogels and Fe_3O_4 nanoparticles exhibited uniform spherical shape, and narrow particle-size distributions. The mean particle size of naked Fe_3O_4 nanoparticles was about 10 nm. TEM proved that microspheres of Fe_3O_4/PAMPS-Na and Fe_3O_4/AMPS/AA were more monodisperse and much smaller than those for Fe_3O_4/AMPS/AM

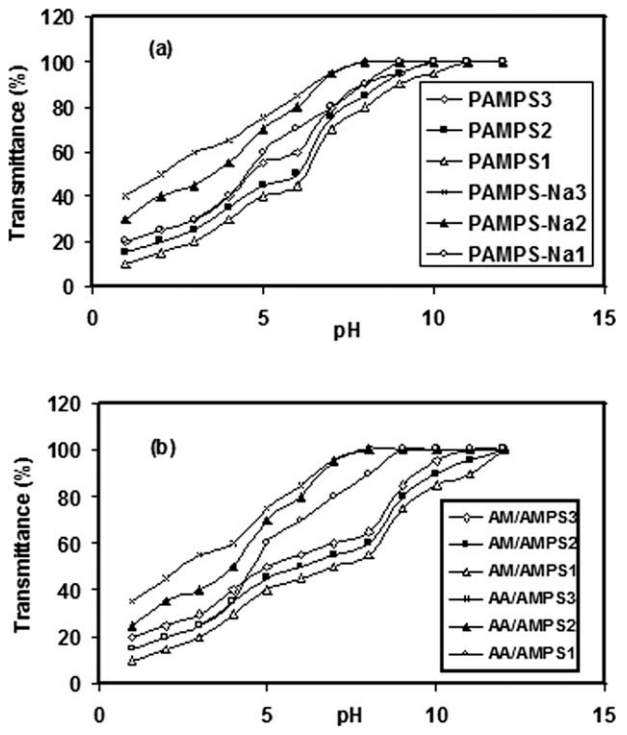

Figure 7 Effect of the pH on the transmittance of crosslinked magnetic (a) Fe3O4-PAMPS and PAMPS-Na; and (b) Fe3O4-AA/AMPS and AM/AMPS nanogels.

nanogels. The presence of both SO_3^{-2} and COO^- ionic groups in the structure of AMPS/AA nanogels increased their dispersion in the aqueous medium which increased the formation of monodispersed nanogels. The transmittance increased for PAMPS-Na> AA/AMPS >PAMPS > AM/AMPS. This can be attributed to residual carboxyl groups of AA chains and sulfonate groups of AMPS deprotonate by increasing the pH; the particles become more compact; therefore, the ratio of particle size and the wavelength changes caused rising transmittance values.

References

1. Wang, P.; Lee, C.; Young, T. J Polym Sci Part A Polym Chem 2005, 43, 1342.
2. Bocanegra-Diaz, A.; Mohallem, N. D. S.; Novak, M. A.; Sinisterra, R. D. J Magn Magn Mater 2004, 272, 2395.
3. Hong, R. Y.; Pan, T. T.; Li, H. Z. J Magn Magn Mater 2006, 303, 60.
4. Yu, L. Q.; Zheng, L. J.; Yang, J. X. Mater Chem Phys 2000, 66, 6.
5. Gun'ko, Y. K.; Cristmann, U.; Kessler, V. G. Eur J Inorg Chem 2002, 5, 1029.
6. Shchukin, D. G.; Radtchenko, I. L.; Sukhorukov, G. B. Mater Lett 2003, 57, 1743.
7. Butter, K.; Philipse, A. P.; Vroege, G. J. J Magn Magn Mater 2002, 252, 1.
8. Wang, J.; Zhang, K.; Chen, Q. W. J Cryst Growth 2004, 266, 500.
9. Wunderbaldinger, P.; Josephson, L.; Weissleder, R. Bioconjugate Chem 2002, 13, 264.
10. Nunes, J. S.; Vasconcelos, C. L.; Cabral, F. A. O.; Araujo, J. H.; Pereira, M. R.; Fonseca, J. L.C. Polymer 2006, 47, 7646.
11. Massia, S. P.; Stark, J.; Letbetter, D. S. Biomaterials 2000, 21, 2253.
12. Wang, Y.; Wang, X.; Luo, G.; Dai, Y. Bioresource Tehcnol 2008, 99, 3881.
13. Zhu, L.; Ma, J.; Jia, N.; Zhao, Y.; Shen, H. Colloid Surf B 2009, 68, 1.
14. Zhi, J.; Wang, Y.; Lu, Y.; Ma, J.; Luo, G. React Funct Polym 2006, 66, 1552.
15. Yuan, Q.; Venkatasubramanian, R.; Hein, S.; Misra, R. D. K. Acta Biomater 2008, 4, 1024.
16. Zhao, D.; Wang, X.; Zeng, X.; Xia, Q.; Tang, J. J Alloy Comp 2009, 477, 739.
17. Cao, J.; Wang, Y.; Yu, J.; Xia, J.; Zhang, C.; Yin, D.; Hafeli, U. O. J Magn Magn Mater 2004, 277, 165.
18. Lu, A. H.; Salabas, E. L.; Schuth, F. Angew Chem Int Ed 2007, 46, 1222.
19. Welo, L. A.; Baudisch, O. Philosophical Mag Series 6 1925, 50, 399.
20. Qu, S. C.; Yang, H. B.; Ren, D. W.; Kan, S. H.; Zou, G. T.; Li, D. M. J Colloid Interface Sci 1999, 215, 190.
21. Kang, Y. S.; Risbud, S.; Rabolt, J. F.; Stroeve, P. Chem Mater 1996, 8, 2209.
22. Munshi, N.; De, T. K.; Maitra, A. J Colloid Interface Sci 1997, 190, 387.
23. Yanbao, G.; Mingxia, F.; Feng, G.; Jun, H.; Shunying, L.; Shufang, L.; Jiahui, Y.; Jin, H. Colloids Surfaces B: Biointerfaces 2009, 71, 243.
24. Wong, J. E.; Richtering, W. Prog Colloid Polym Sci 2006, 133, 45.
25. Nayak, S.; Lee, H.; Chmielewski, J.; Lyon, L. A. J Am Chem Soc 2004, 126, 10258.
26. Grabarek, Z.; Gergely, J. Anal Biochem 1990, 185, 131.
27. Sivokhin, A. P.; Kazantsev, O. A.; Shirshin, K. V. Russian J Appl Chem 2007, 80, 1394.
28. Rahimi, M.; Yousef, M.; Cheng, Y.; Meletis, E. I.; Eberhart, R. C.; Nguyen, K. J Nanosci Nanotechnol 2009, 9, 4128.
29. Kabiri, K.; Zohuriaan-Mehr, M. J.; Mirzadeh, H.; Kheirabadi, M. J Polym Res 2010, 17, 203.
30. Atta, A. M.; El-Azabawy, O. E.; Ismail, H. S.; Hegazy, M. A. Corrosion Sci 2011, 53, 1680.
31. Hong, R. Y.; Pan, T. T.; Han, Y. P.; Li, H. Z.; Ding, J.; Han, S. J. J Magn Magn Mater 2007, 310, 37.
32. Corrias, A.; Ennas, G.; Musinu, A.; Marongiu, G.; Paschina, G. Chem Mater 1993, 5, 1722.
33. Hua, L.; Rongmo, L.; Erik, B. J Appl Phys 2007, 101, 114.
34. Rego, J. M.; Huglin, M. B.; Gooda, S. R. Br Polym J 1990, 23, 333.